Mechanical integrators for the inverse dynamics of dissipative multibody systems

S. Uhlar[1], P. Betsch[2]

[1] *Chair of Computational Mechanics, Department of Mechanical Engineering, University of Siegen, Germany, uhlar@imr.mb.uni-siegen.de*

[2] *Chair of Computational Mechanics, Department of Mechanical Engineering, University of Siegen, Germany, betsch@imr.mb.uni-siegen.de*

Abstract

A unified approach for the description of multibody systems is presented, relying on a rotationless formulation for rigid bodies. The set of differential algebraic equations governing the motion of multibody dynamics does not only beneficially offer the design of energy-momentum schemes but it also bears the advantage to be extended by vital modeling features. In this spirit we present within this contribution the modeling of frictional phenomena such as joint friction and the incorporation of control constraints. Both features rely on a specific augmentation technique which incorporates rotational degrees of freedom into the rotationless formulation. The example of a partially controlled movement of a free floating parallel platform afflicted with joint friction will demonstrate the performance of the newly developed energy-momentum consistent scheme.

Keywords: Differential algebraic equations, multibody systems, dissipation, energy consistency, control.

1 INTRODUCTION

The present work relies on a specific rotationless formulation of multibody dynamics. The configuration of each individual rigid body is characterized by a set of redundant coordinates. The corresponding equations of motion assume the form of differential-algebraic equations (DAEs). Due to the fact that the mass matrix is constant, the DAEs have a particularly simple structure which turns out to be highly beneficial to the design of conserving time-stepping schemes. Conserving schemes, in particular energy-momentum schemes and their energy decaying variants, are well-known to provide enhanced numerical stability properties (see, for example, Gonzalez & Simo [10] or Ibrahimbegović et al. [12]). At the same time, the DAE structure offers the benefit to simply append new modeling features. In this connection we will outline the coordinate augmentation technique, the modeling of joint friction and the incorporation of control constraints.

The coordinate augmentation technique was first applied to planar multibody systems in Betsch and Uhlar [4], see also [22]. This feature can be regarded as a modeling technique since it enables the introduction of any arbitrary value, e.g. a relative joint angle. It also forms the base for the modeling of joint friction, since the joint friction torque commonly depends on the relative joint angle.

For the modeling of dissipation, more precisely joint friction, we rely on thermodynamic models arising from the constitutive modeling in material mechanics. These models have the advantage of calculating the correct amount of dissipation, while retaining the ability of augmenting the models in such a way that they can reproduce experimental results by parameter identification. The ideas to this approach go back to the modeling of viscoelastic material behavior for dynamics, introducing an energy-consistent integration scheme due to Gross [11]. For finite elasto-plasto-dynamics energy consistent schemes have been developed by Noels et al. [17], Mohr et al. [14, 15, 16] or Armero [1]. We will basically follow these ideas and break them down to the 1D case, and finally derive an energy-momentum consistent time stepping scheme.

We outline in the following that the present approach to the simulation of multibody dynamics can easily accommodate control (or servo) constraints. Control constraints can be directly appended to the present DAEs. This makes possible to partially specify the motion of a multibody system. In particular, inverse dynamics problems can be dealt with in the present simulation framework. It turns out that the underlying rotationless description along with the coordinate augmentation technique yields simple-structured control contributions to the DAEs. In particular, the Jacobian associated with the control constraints is typically of Boolean (or binary) form. This is in contrast to formulations in terms of generalized coordinates, see Blajer and Kolodziejczyk [5] and the references therein.

An outline of the rest of the paper is as follows. Section 2 contains the continuous and discrete equations of motion governing the motion of multibody systems. The advocated rotationless formulation along with the coordinate augmentation is presented in Section 3. The modeling of dissipation, applying a plasticity model for joint friction will be outlined in Section 4, rendering an energy-consistent time integration scheme. Additionally, we show that control (or servo) constraints can be easily appended to the present DAEs. The conserving numerical integration of the

DAEs is described in Section 5. The performance of the presented time stepping scheme along with all addressed features is carried out with the example of a free floating parallel platform in Section 6.

2 GOVERNING EQUATIONS OF MOTION

In this section we outline the equations of motion which provide a uniform framework for the rotationless formulation of multibody dynamics. In the first instance we focus only on discrete mechanical systems which are holonomic and scleronomic (extensions for the rheonomic case can be found in Section 5). Accordingly, the equations of motion assume the form

$$\begin{aligned} \dot{\boldsymbol{q}} - \boldsymbol{v} &= \boldsymbol{0} \\ \boldsymbol{M}\dot{\boldsymbol{v}} + \nabla V(\boldsymbol{q}) + \boldsymbol{G}^T(\boldsymbol{q})\boldsymbol{\lambda} &= \boldsymbol{0} \\ \boldsymbol{\Phi}(\boldsymbol{q}) &= \boldsymbol{0} \end{aligned} \tag{1}$$

Here, $\boldsymbol{q}(t) \in \mathbb{R}^n$ specifies the configuration of the mechanical system at time t, and $\boldsymbol{v}(t) \in \mathbb{R}^n$ is the velocity vector. Together $(\boldsymbol{q}, \boldsymbol{v})$ form the vector of state space coordinates (see, for example, Rosenberg [18]). Here, $V(\boldsymbol{q}) \in \mathbb{R}$ is a potential energy function and $\boldsymbol{\Phi}(\boldsymbol{q}) \in \mathbb{R}^m$ is a vector of geometric constraint functions, while $\boldsymbol{G} = D\boldsymbol{\Phi}(\boldsymbol{q}) \in \mathbb{R}^{m\times n}$ is the constraint Jacobian and $\boldsymbol{\lambda} \in \mathbb{R}^m$ a vector of multipliers which specify the relative magnitude of the constraint forces. In the description above, it is tacitly assumed that the m constraints are independent.

Due to the presence of holonomic (or geometric) constraints $(1)_3$, the configuration space of the system is given by

$$\mathsf{Q} = \{\boldsymbol{q}(t) \in \mathbb{R}^n | \, \boldsymbol{\Phi}(\boldsymbol{q}) = \boldsymbol{0}\} \tag{2}$$

The equations of motion (1) form a set of index-3 differential-algebraic equations (DAEs) (see, for example, Kunkel and Mehrmann [13]). They can be directly derived from the classical Lagrange's equations.

2.1 Discretization of the DAEs, Basic-Energy-Momentum Scheme

The discretization of the continuous equations of motion (1) is carried out by applying the Basic-Energy-Momentum (**BEM**) scheme introduced in [4]. To summarize, we obtain the following set of discretized algebraic equations for the time interval $[t_n, t_{n+1}]$ with the step size $\Delta t = t_{n+1} - t_n$

$$\begin{aligned} \boldsymbol{q}_{n+1} - \boldsymbol{q}_n &= \frac{\Delta t}{2}\,(\boldsymbol{v}_n + \boldsymbol{v}_{n+1}) \\ \boldsymbol{M}\,(\boldsymbol{v}_{n+1} - \boldsymbol{v}_n) &= -\Delta t\,\bar{\nabla} V(\boldsymbol{q}_n, \boldsymbol{q}_{n+1}) - \Delta t\,\bar{\mathbf{G}}(\boldsymbol{q}_n, \boldsymbol{q}_{n+1})^T\boldsymbol{\lambda} \\ \boldsymbol{\Phi}(\boldsymbol{q}_{n+1}) &= \boldsymbol{0} \end{aligned} \tag{3}$$

The algorithmic conservation properties of the **BEM** scheme are linked to the notion of a discrete gradient (or derivative) of a function $f : \mathbb{R}^n \mapsto \mathbb{R}$. In the present work $\bar{\nabla} f(\boldsymbol{q}_n, \boldsymbol{q}_{n+1})$ denotes the discrete gradient of f [8, 9]. It is worth mentioning that if f is at most quadratic then the discrete gradient coincides with the standard gradient evaluated in the mid-point configuration $\boldsymbol{q}_{n+1/2} = (\boldsymbol{q}_n + \boldsymbol{q}_{n+1})/2$, that is, in this case $\bar{\nabla} f(\boldsymbol{q}_n, \boldsymbol{q}_{n+1}) = \nabla f(\boldsymbol{q}_{n+1/2})$.

Remark 2.1 *Although the rotationless formulation is accompanied with a large number of unknowns, a reduction can be achieved by applying the size reduction technique proposed in [2, 3, 4].*

3 ROTATIONLESS FORMULATION OF THE RIGID BODY

The configuration of a rigid body in the three-dimensional Euclidean space is characterized by the placement of its center of mass $\boldsymbol{\varphi}(t) \in \mathbb{R}^3$ and a right-handed body frame $\{\boldsymbol{d}_I\}$, $\boldsymbol{d}_I(t) \in \mathbb{R}^3$ ($I = 1, 2, 3$), which specifies the orientation of the body (Fig. 1). The vectors $\boldsymbol{d}_I$ will be

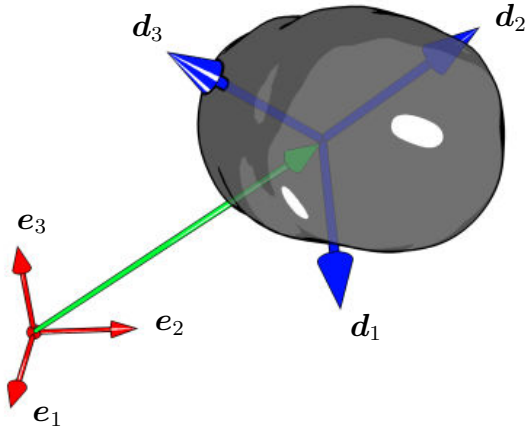

Figure 1: The rigid body – rotationless description.

occasionally called directors. Let $\boldsymbol{X} = X_i\, \boldsymbol{e}_i$[§] be a material point which belongs to the reference configuration $V \subset \mathbb{R}^3$ of the rigid body. The spatial position of $\boldsymbol{X} \in V$ at time t relative to an inertial Cartesian basis $\{\boldsymbol{e}_I\}$ can now be characterized by

$$\boldsymbol{x}(\boldsymbol{X}, t) = \boldsymbol{\varphi}(t) + X_i\, \boldsymbol{d}_i(t) \tag{4}$$

Obviously, the configuration of the rigid body can be described by the following vector of redundant coordinates ($n = 12$)

$$\boldsymbol{q} = \begin{bmatrix} \boldsymbol{\varphi}^T & \boldsymbol{d}_1^T & \boldsymbol{d}_2^T & \boldsymbol{d}_3^T \end{bmatrix}^T \tag{5}$$

Redundancy implies additional constraint equations, which in this case reflect the orthonormality of the director frame for all times. Thus this leads to $m = 6$ independent internal constraints with associated constraint functions

$$\boldsymbol{\Phi}_{int}(\boldsymbol{q}) = \begin{bmatrix} \boldsymbol{d}_1^T \boldsymbol{d}_1 - 1 & \boldsymbol{d}_2^T \boldsymbol{d}_2 - 1 & \boldsymbol{d}_3^T \boldsymbol{d}_3 - 1 & \boldsymbol{d}_1^T \boldsymbol{d}_2 & \boldsymbol{d}_1^T \boldsymbol{d}_3 & \boldsymbol{d}_2^T \boldsymbol{d}_3 \end{bmatrix}^T \tag{6}$$

As outlined in detail in [3] we distinguish between internal and external constraint equations, where external constraints handle joint connections, linking rigid bodies.
The kinetic energy can be expressed as $1/2 \boldsymbol{v}^T\, \boldsymbol{M}\, \boldsymbol{v}$, where in contrast to other coordinates (e.g. Euler angles, quaternions), the mass matrix is constant and has a diagonal structure. Specifically it

[§]In this work the summation convention applies to repeated lower case Roman indices.

is given by

$$\boldsymbol{M} = \begin{bmatrix} \mathcal{M}\,\boldsymbol{I} & \mathbf{0} & \mathbf{0} & \mathbf{0} \\ \mathbf{0} & \mathcal{E}_1\boldsymbol{I} & \mathbf{0} & \mathbf{0} \\ \mathbf{0} & \mathbf{0} & \mathcal{E}_2\boldsymbol{I} & \mathbf{0} \\ \mathbf{0} & \mathbf{0} & \mathbf{0} & \mathcal{E}_3\boldsymbol{I} \end{bmatrix} \tag{7}$$

where $\boldsymbol{I}$ and $\mathbf{0}$ are the 3×3 identity and zero matrices. $\mathcal{M}$ denotes the total mass of the rigid body and $\mathcal{E}_I$ (I = 1, 2, 3) are the principal values of the convected Euler tensor [4].

3.1 Coordinate augmentation

In this chapter we briefly recapitulate the coordinate augmentation technique presented in [4] since it plays a major role within the present contribution. As already outlined in the introduction, the rotationless formulation does not concern rotational DOF. Yet these are of major importance for the modeling of real mechanical systems, e.g. for implementing joint torques (see [22]) or joint friction. The introduction of rotational coordinates can be demonstrated clearly with the example of a planar revolute pair as depicted in Fig. 2. First, we extend the configuration vector by the

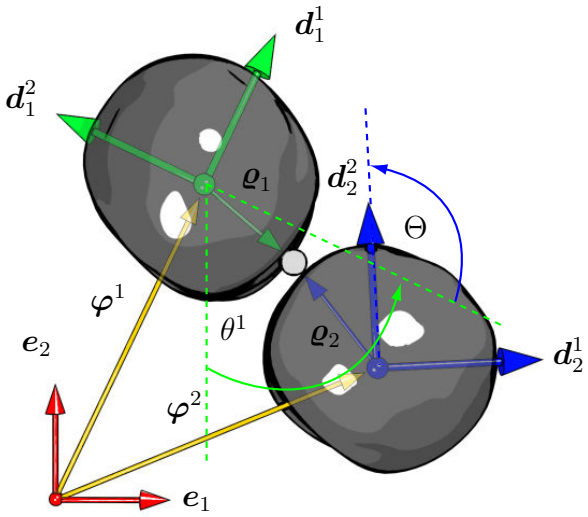

Figure 2: The planar revolute pair.

augmented variable Θ, which then leads to

$$\boldsymbol{q}_{ori} = \begin{bmatrix} \boldsymbol{q}^1 \\ \boldsymbol{q}^2 \end{bmatrix}, \quad \boldsymbol{q} = \begin{bmatrix} \boldsymbol{q}_{ori} \\ \Theta \end{bmatrix} \tag{8}$$

Augmented variables imply additional constraint equations, in this case we obtain

$$\Phi_{aug} = \underbrace{\boldsymbol{d}_2^2 \cdot \boldsymbol{d}_1^1 + \boldsymbol{d}_2^2 \cdot \boldsymbol{d}_2^1}_{\Phi^1_{aug}(\boldsymbol{q}_{ori})} + \underbrace{\sin\Theta - \cos\Theta}_{\Phi^2_{aug}(\Theta)} \tag{9}$$

The corresponding constraint Jacobian in the continuous case yields

$$\boldsymbol{G}_{aug}(\boldsymbol{q}) = \begin{bmatrix} \boldsymbol{G}^1_{aug}(\boldsymbol{q}_{ori}) & G^2_{aug}(\Theta) \end{bmatrix} \tag{10}$$

with

$$\begin{aligned} \boldsymbol{G}^1_{aug}(\boldsymbol{q}_{ori}) &= \begin{bmatrix} \boldsymbol{0}^T & (d_2^2)^T & (\boldsymbol{d}_2^2)^T & \boldsymbol{0}^T & \boldsymbol{0}^T & (\boldsymbol{d}_1^1 + \boldsymbol{d}_2^1)^T \end{bmatrix} \\ G^2_{aug}(\Theta) &= \sin\Theta + \cos\Theta \end{aligned} \tag{11}$$

3.1.1 Discrete constraint Jacobian

As obvious from equation (9), $\Phi^1_{aug}(\boldsymbol{q}_{ori})$ is only quadratic, therefore the associated discrete gradient coincides with the mid-point evaluation of its corresponding constraint Jacobian ($\boldsymbol{G}^1_{aug}((\boldsymbol{q}_{ori})_{n+\frac{1}{2}})$). In contrast to this, the constraint Jacobian of the second part of the augmented constraint equation $\Phi^2_{aug}(\Theta)$ must be evaluated according to

$$\boldsymbol{G}^2_{aug}(\Theta_n, \Theta_{n+1}) = \frac{\Phi^2_{aug}(\Theta_{n+1}) - \Phi^2_{aug}(\Theta_n)}{\Theta_{n+1} - \Theta_n} \tag{12}$$

which can be interpreted as a G-equivariant discrete derivative in the sense of Gonzalez [8].

Remark 3.1 *The augmentation technique is not only restricted to the implementation of rotational DOF, any arbitrary value which is necessary for modeling purpose can be incorporated. In this sense the augmentation technique can be regarded as a modeling technique, e.g. for measuring values.*

4 MODELING OF DISSIPATION

In this section we outline the incorporation of dissipative effects into our multibody framework, followed by the modeling of joint plasticity, based upon [21]. This can be regarded as a thermodynamic consistent model which captures the transient effects of stiction and sliding (see Section 4.2).

4.1 Incorporation of dissipation

The implementation of dissipative effects into the multibody framework presented before, relies on the coordinate augmentation technique outlined in Section 3.1. Since our dissipative model presented within this contribution is one dimensional, acting on original or augmented coordinates, the incorporation is performed by adding an internal force to the equations of motion in the continuous case. This internal force vector has only entries at the corresponding coordinates the dissipation is acting on, therefore in general the continuous equations of motion can be written as

$$\begin{aligned} \dot{\boldsymbol{q}} - \boldsymbol{v} &= \boldsymbol{0} \\ \boldsymbol{M}\dot{\boldsymbol{v}} + \nabla V(\boldsymbol{q}) + \boldsymbol{G}^T(\boldsymbol{q})\boldsymbol{\lambda} + \boldsymbol{F}_{int} &= \boldsymbol{0} \\ \boldsymbol{\Phi}(\boldsymbol{q}) &= \boldsymbol{0} \end{aligned} \tag{13}$$

To obtain a consistent time stepping scheme for dissipative multibody systems, we need to discretize the set of equations above. First we apply the **BEM**-scheme presented in Section 2.1,

whereby we seek an algorithmic force evaluation which satisfies the discrete consistency condition $R := H_{n+1} - H_n + \Delta\mathcal{D} = 0$, where $H = T + V$ is the Hamiltonian function and $\mathcal{D}$ the dissipation (for further details see [21]). In general we obtain the following set of discretized algebraic equations

$$\begin{aligned} \boldsymbol{q}_{n+1} - \boldsymbol{q}_n &= \frac{\Delta t}{2}\,(\boldsymbol{v}_n + \boldsymbol{v}_{n+1}) \\ \boldsymbol{M}\,(\boldsymbol{v}_{n+1} - \boldsymbol{v}_n) &= -\Delta t\,\bar{\nabla} V(\boldsymbol{q}_n, \boldsymbol{q}_{n+1}) - \Delta t\,\bar{\mathbf{G}}(\boldsymbol{q}_n, \boldsymbol{q}_{n+1})^T \boldsymbol{\lambda} + \Delta t\,\boldsymbol{F}_{int}^{alg} \\ \boldsymbol{\Phi}(\boldsymbol{q}_{n+1}) &= \mathbf{0} \end{aligned} \tag{14}$$

The above scheme represents an extension of the **BEM**-scheme (3) and will be referred to as the **E**nergy-**M**omentum-**C**onsistent (**EMC**) scheme. The character of $\boldsymbol{F}_{int}^{alg}$ will be revealed in detail within the next section, since it depends on a respective dissipative model.

4.2 Plasticity model

For modeling the characteristics of stiction and sliding, we choose in the first instance a rheological model of perfect plasticity. In order to apply this model to a dynamical problem, we introduce a friction-element oscillator [14] and discuss all necessary steps with this example. All required basic notations of perfect plasticity can be found in [20].

4.2.1 Friction-Element-Oscillator

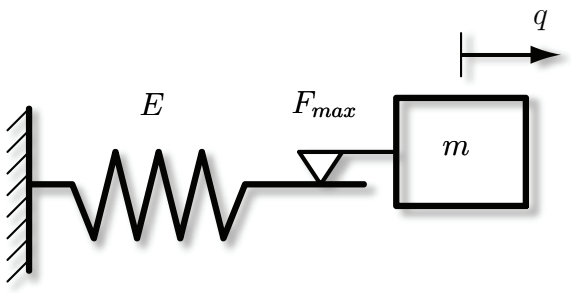

Figure 3: Friction element oscillator.

Following the lines of [14], we derive the equations of motion, show how to implement our plasticity model and how to perform a consistent integration. Starting with the additive split of the displacement

$$q = q^e + q^p \quad \Rightarrow \quad q^e = q - q^p \tag{15}$$

The equations of motion can directly be written as

$$m\,\ddot{q} + F_{int} + F_{ext} = 0 \tag{16}$$

Assuming a linear spring characteristic for the pure elastic case, the free energy function yields

$$\Psi(q^e, E) = \frac{1}{2}\,E\,(q^e)^2 = \frac{1}{2}\,E\,(q - q^p)^2 \tag{17}$$

A differentiation of the free energy function wrt q^e yields the internal force

$$F_{int} = \partial_{q^e} \Psi = E\, q^e = E\,(q - q^p) \tag{18}$$

The determination when plastic slip occurs can be stated by defining the yield condition

$$\Phi(F_{int}) = |F_{int}| - F_{max} \leq 0 \tag{19}$$

It is obvious from the equation above that plastic deformation only occurs if $|F_{int}| = F_{max}$, leading to the following evolution equation (see [20])

$$\dot{q}^p = \dot{\lambda}\, \frac{F_{int}}{|F_{int}|} = \dot{\lambda}\, \text{sign}\, F_{int} \tag{20}$$

While the loading and unloading conditions can be written as

$$\Phi(F_{int}) < 0 \quad \dot{\lambda} = 0 \quad \text{and} \quad \Phi(F_{int}) = 0 \quad \dot{\lambda} > 0 \tag{21}$$

leading to the Kuhn-Tucker complementary condition

$$\dot{\lambda}\, \Phi(F_{int}) = 0 \tag{22}$$

4.2.2 Energy-consistent disretization

The discretization of the equations of motion in (16) relies again on the mid-point rule

$$\begin{aligned} q_{n+1} - q_n &= \frac{\Delta\, t}{2}\,(v_{n+1} + v_n) \\ m\,(v_{n+1} - v_n) + \Delta t\, F_{int}(1/2) + \Delta t\, F_{ext}(1/2) &= 0 \end{aligned} \tag{23}$$

The rheological model is reflected in the internal force F_{int}. A mid-point evaluation of F_{int} does not yield a consistent integration. We need to apply an algorithmic force evaluation according to [21]. For the plasticity model the dissipation yields

$$\mathcal{D} = F_{int}\, \dot{q}^p \tag{24}$$

or incrementaly

$$\Delta \mathcal{D} = \Delta\, \lambda\, F_{max} \tag{25}$$

The algorithmic force can be expressed according to [21] as

$$F_{int}^{alg} = \frac{\Psi_2 - \Psi_1}{q_2 - q_1} + \frac{\Delta \mathcal{D}}{q_2 - q_1} \tag{26}$$

Substituting $F_{int}(1/2)$ in Equation (23) by the algorithmic force evaluation, yields a consistent integration scheme for the friction element oscillator. This can be directly applied to augmented joint coordinates.

5 INCORPORATION OF CONTROL CONSTRAINTS

For the introduction of control constraints we rely on the set of DAEs as presented in 3. As outlined in the Introduction one of the benefits of the DAE structure is the simple extension of the scheme by additional constraints. These control constraints can be appended in a straightforward way. This introduction is accompanied with a corresponding constraint Jacobian according to

$$\begin{aligned} \dot{\boldsymbol{q}} &= \boldsymbol{v} \\ \boldsymbol{M}\dot{\boldsymbol{v}} &= -\nabla V(\boldsymbol{q}) - \boldsymbol{G}^T(\boldsymbol{q})\boldsymbol{\lambda} - \boldsymbol{B}^T\boldsymbol{u} \\ \boldsymbol{0} &= \boldsymbol{b}(\boldsymbol{q}) - \boldsymbol{\gamma}(t) \\ \boldsymbol{0} &= \boldsymbol{\Phi}(\boldsymbol{q}) \end{aligned} \tag{27}$$

In contrast to Equation (1) we find the new algebraic constraints in $(1)_3$, playing the role of control (or servo) constraints. In the rotationless formulation $\boldsymbol{b} : \mathbb{R}^n \mapsto \mathbb{R}^{m_c}$ is typically linear (m_c denotes the number of control constraints). Since we confine our attention to standard rheonomic constraints, the input transformation matrix $\boldsymbol{B} = D\boldsymbol{b}(\boldsymbol{q}) \in \mathbb{R}^{m_c \times n}$ is constant. The associated Lagrange multipliers $\boldsymbol{u} \in \mathbb{R}^{m_c}$ play the role of control inputs. We refer to Blajer and Kolodziejczyk [5] for a more general framework of control constraints.

5.1 Conserving integration of the DAEs

A corresponding energy-momentum (EM) conserving time-stepping scheme with mixed holonomic and control constraints can be obtained by a direct discretization of the DAEs (27) and yields

$$\begin{aligned} \boldsymbol{q}_{n+1} - \boldsymbol{q}_n &= \frac{\Delta t}{2}\left(\boldsymbol{v}_n + \boldsymbol{v}_{n+1}\right) \\ \boldsymbol{M}\left(\boldsymbol{v}_{n+1} - \boldsymbol{v}_n\right) &= -\Delta t\left\{\bar{\nabla} V(\boldsymbol{q}_n, \boldsymbol{q}_{n+1}) + \mathbf{G}(\boldsymbol{q}_n, \boldsymbol{q}_{n+1})^T\bar{\boldsymbol{\lambda}} + \boldsymbol{B}^T\bar{\boldsymbol{u}}\right\} \\ \boldsymbol{0} &= \boldsymbol{b}(\boldsymbol{q}_{n+1}) - \boldsymbol{\gamma}(t_{n+1}) \\ \boldsymbol{0} &= \boldsymbol{\Phi}(\boldsymbol{q}_{n+1}) \end{aligned} \tag{28}$$

The scheme above is similar to the BEM-scheme given above, but is extended by the newly appended constraints. The application of Equations (28) makes possible the determination of the control inputs $\bar{\boldsymbol{u}} \in \mathbb{R}^{m_c}$ in a straightforward way, which is in contrast to typical procedures while dealing with inverse dynamics problems (see e.g. [6, 7, 19]).

6 NUMERICAL EXAMPLE

Our numerical example deals with a free floating (no gravity) planar parallel manipulator. The system at hand has six degrees of freedom (namely the three angles of rotation Θ_1, Θ_2, Θ_3 and the 3 DOF of the platform body 8). The intention is to let body number 7 move upon a prescribed trajectory, while we actuate the joints Θ_1, Θ_2 and Θ_3. This means that we deal with an underactuated control problem. This example was studied in detail in [22], where all modeling steps concerning the implementation and the augmentation can be found. We confine our attention on the implementation of joint friction, applying the presented plasticity model. The goal is to point out how important an accurate modeling of joint friction for control problems is. The results will compare the necessary actuation torques for the conservative case, with the values obtained in the friction afflicted case.

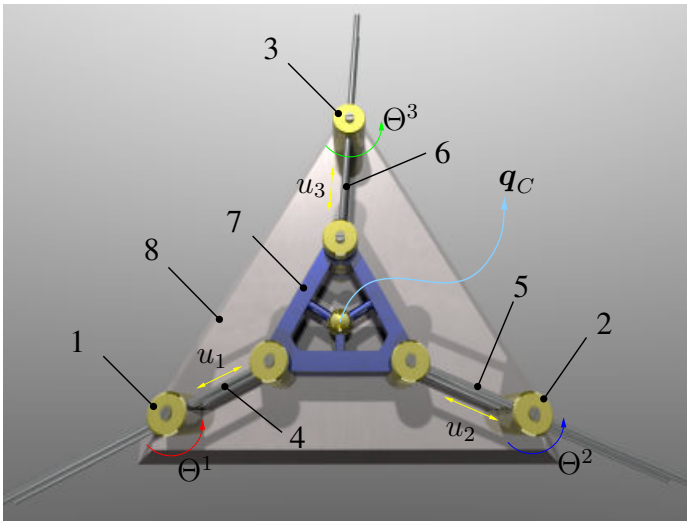

Figure 4: Schematics of the RPR-manipulator.

The system we want to investigate is depicted in Fig. 4. In contrast to the implementation in [22], we activate joint friction in the revolute joints (acting on Θ_1, Θ_2, Θ_3). For the simulation we choose the following values for the plasticity joint friction model: a spring stiffness of $E = 350$ and a breakaway force of $F_{max} = 50$. All other parameters concerning masses, inertia and geometry coincide with the values used in [22], the initial configuration and the prescribed figure-8 trajectory are provided in detail in the reference cited before (all values specified are provided in SI-units).

Figure 5b shows the evolution of the augmented angles Θ^I, $I = 1, 2, 3$, while Fig. 5a shows the

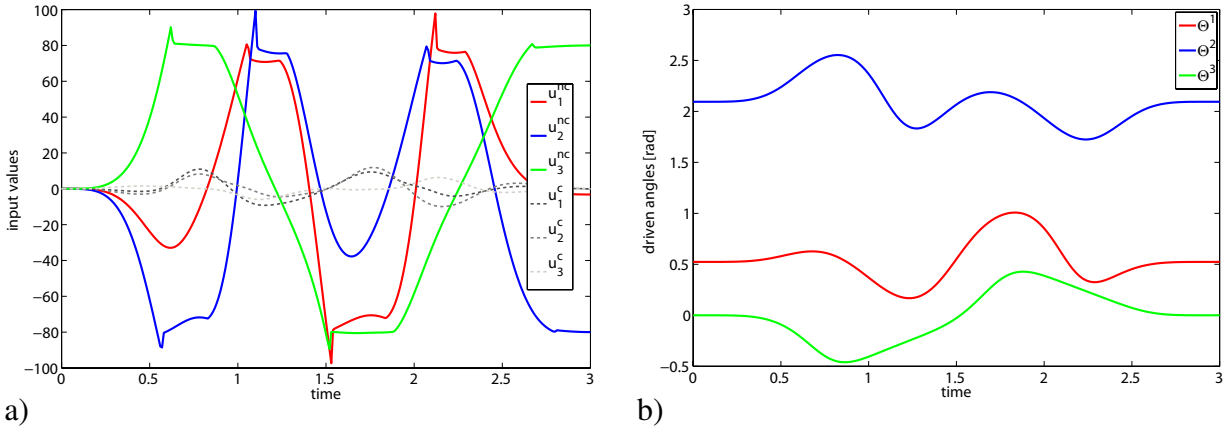

a) b)

Figure 5: a) Comparisson of necessary inputs for the non-conservative^{nc} and conservative^{c} case, b) Evolution of the driven angles.

comparison of the necessary driving torques, once with activated joint friction (nc) and once for

the conservative case (c). Obviously joint friction has a major influence on control problems. Depending on the values chosen for the friction model, the driving torques exceed notably the values for the conservative case. We choose a time step size of $\Delta t = 0.01$.

7 CONCLUSIONS

The present contribution outlined the incorporation of dissipation and the modeling of control problems within a rotationless formulation for rigid body dynamics, rendering an energy-consistent time stepping scheme. Concerning the modeling of dissipation we showed that only thermodynamic consistent models form the base for the construction of a mechanical integrator. The introduction of control constraints was performed by simply extending the DAE-set by additional control constraints accompanied with a constraint Jacobian of Boolean type. This leads to a unified approach for solving inverse dynamics problems in one step, which is in contrast to other common approaches. The performance of our scheme was clearly demonstrated with the example of a free floating manipulator, pointing out the importance of an adequate model for joint friction and its influence on the corresponding control inputs.

REFERENCES

[1] F. Armero. Energy-dissipative momentum-conserving time-stepping algorithms for finite strain multiplicative plasticity. *Comput. Methods Appl. Mech. Engrg.*, 195:4862–4889, 2006.

[2] P. Betsch. The discrete null space method for the energy consistent integration of constrained mechanical systems. Part I: Holonomic constraints. *Comput. Methods Appl. Mech. Engrg.*, 194(50-52):5159–5190, 2005.

[3] P. Betsch and S. Leyendecker. The discrete null space method for the energy consistent integration of constrained mechanical systems. Part II: Multibody dynamics. *Int. J. Numer. Methods Eng.*, 67(4):499–552, 2006.

[4] P. Betsch and S. Uhlar. Energy-momentum conserving integration of multibody dynamics. *Multibody System Dynamics*, 17(4):243–289, 2007.

[5] W. Blajer and K. Kołodziejczyk. A geometric approach to solving problems of control constraints: Theory and a DAE framework. *Multibody System Dynamics*, 11(4):343–364, 2004.

[6] R. Featherstone. *Rigid body dynamics algorithms*. Springer-Verlag, 2008.

[7] T. Geike and J. McPhee. Inverse dynamic analysis of parallel manipulators with full mobility. *Mechanism and Machine Theory*, 38:549–562, 2003.

[8] O. Gonzalez. Time integration and discrete Hamiltonian systems. *J. Nonlinear Sci.*, 6:449–467, 1996.

[9] O. Gonzalez. Mechanical systems subject to holonomic constraints: Differential-algebraic formulations and conservative integration. *Physica D*, 132:165–174, 1999.

[10] O. Gonzalez and J.C. Simo. On the stability of symplectic and energy-momentum algorithms for non-linear Hamiltonian systems with symmetry. *Comput. Methods Appl. Mech. Engrg.*, 134:197–222, 1996.

[11] M. Groß and P. Betsch. Energy-momentum consistent finite element discretisation of dynamic finite deformation isothermal viscoelasticity. preprint.

[12] A. Ibrahimbegović, S. Mamouri, R.L. Taylor, and A.J. Chen. Finite element method in dynamics of flexible multibody systems: Modeling of holonomic constraints and energy conserving integration schemes. *Multibody System Dynamics*, 4(2-3):195–223, 2000.

[13] P. Kunkel and V. Mehrmann. *Differential-Algebraic Equations*. European Mathematical Society, 2006.

[14] R. Mohr. *Consistent Time-Integration of Finite Elasto-Plasto-Dynamics*. Phd thesis, University of Kaiserslautern, 2008.

[15] R. Mohr, A. Menzel, and P. Steinmann. A consistent time fe-method for large strain elasto-plasto-dynamics. *Comput. Methods Appl. Mech. Engrg.*, 197:3024–3044, 2008.

[16] R. Mohr, S. Uhlar, A. Menzel, and P. Steinmann. Time-fe methods for the nonlinear dynamics of constrained inelastic systems. *IUTAM Bookseries*, In IUTAM Symposium on Theoretical, Modelling and Computational Aspects of Inelastic Media:275–285, 2008.

[17] L. Noels, L. Stainier, and J.P. Ponthot. An energy-momentum conserving algorithm for non-linear hypoelastic constitutive models. *Int. J. Numer. Methods Eng.*, 59:83–114, 2004.

[18] R.M. Rosenberg. *Analytical dynamics of discrete systems*. Plenum Press, 1977.

[19] S.K. Saha and W.O. Schiehlen. Recursive kinematics and dynamics for parallel structured closed loop multibody systems. *Mech. Struct. & Mach.*, 29(2):143–175, 2001.

[20] J.C. Simo and T.J.R. Hughes. *Computational Inelasticity*. Springer-Verlag, New York, 1998.

[21] S. Uhlar and P. Betsch. Energy consistent integration of dissipative multibody systems. *preprint*.

[22] S. Uhlar and P. Betsch. Conserving integrators for parallel manipulators. In J.-H. Ryu, editor, *Parallel Manipulators*, chapter 5, pages 75–108. I-Tech Education and Publishing, www.books.i-techonline.com, Vienna, Austria, 2008.